International Geology Review, Vol. 48, 2006, p. 311–328.

Early Mesozoic, Post-collisional Shoshonitic Lamprophyres along the Western Margin of the South China Orogen: Geochemical Characteristics and Tectonic Implications

XIN-QUAN LIANG,[1] WEI-MING FAN, YUE-JUN WANG, AND XIAN-HUA LI

Key Laboratory of Isotope Geochronology and Geochemistry, Guangzhou Institute of Geochemistry, Chinese Academy of Sciences, P.O. Box 1131, Guangzhou 510640, China

Abstract

The Anhua-Xupu shoshonitic lamprophyres, emplaced along the western margin of the South China orogen (Cathaysian block), formed about 207 Ma. They are characterized by high K_2O/Na_2O ratios (0.84–1.72), high $K_2O + Na_2O$ contents (>4.33–6.41%), low TiO_2 contents (0.54–1.21%), variable but high Al_2O_3 contents (13.32–16.28%), strong enrichments in LILE and LREE, and distinct depletions in HFSE (such as Nb, Ta, and Ti) with no Eu anomalies. The rocks possess highly initial radiogenic $^{87}Sr/^{86}Sr$ ratios (0.721565–0.722292) and nonradiogenic $^{143}Nd/^{144}Nd$ ratios (0.511836–0.511869), corresponding to $\varepsilon_{Nd}(t)$ = –9.81 to –10.45. Such geochemical characteristics are comparable to the Åva lamprophyres in southern Finland and Russian Karelia, the melilite-bearing rocks from the Montefiascone Volcanic Complex (Roman Magmatic Province), and the Damavand shoshonitic volcanics (Central Alborz, northern Iran). Geochemical and isotopic signatures shown by the Anhua-Xupu primary magmas require a clinopyroxene- and phlogopite-rich mantle source, whereas partial melting of a veined lithospheric mantle accounts for the occurrence of different primary magmas characterized by relatively constant Sr- and Nd-isotopic compositions. Ages of the depleted mantle Nd-model (1.30–1.37 Ga) implies that mantle enrichment may have been related to Proterozoic suturing of the Yangtze and Cathaysian blocks. Considering the regional tectonic evolution, we suggest that the generation of these shoshonitic lamprophyres was a product of post-collisional intralithospheric extension during Early Mesozoic time.

Introduction

THE ANHUA-XUPU AREA, lying on the western margin of the South China orogen, also called the Cathaysian Block (Huang, 1977; Wang, 1986) (Fig. 1A), is a of key region for studying the tectonic evolution of SE Asia after amalgamation between the two crustal blocks. The Banxi Group epimetamorphic clastic rocks and Sinian tillite crop out along the suture zone between the Yangtze and Cathaysian blocks (Fig. 1A). Over the past 20 years, a number of models have been postulated to explain the tectonic evolution of the South China Block and the petrogenesis of the associated Mesozoic igneous rocks (Ren et al., 1980; Wang et al., 1986; Hsü et al., 1988; Chen et al., 1993; Jia, 1994; Liang et al., 1999; Zhou and Li, 2000). An extensional regime is now favored for its Late Mesozoic tectonic evolution (e.g., Li, 2000; Wang et al., 2003a). However, the tectonic setting during the Early Mesozoic in this region remains hotly debated. Hypotheses, such as an Andean-type active continental margin, an Alpine-type collision belt, or lithosphere subduction with underplating of mafic magma, suggest that the tectonic evolution of the South China Block was related to subduction/collision (e.g., Hsü et al., 1990; Faure et al., 1996; Chen et al., 1993, and reference therein). However, other scenarios postulate that it was related to intraplate lithospheric extension and thinning (Guo et al., 1997; Li, 2000; Wang Y. J. et al., 2001, 2003a; and reference therein).

Recent studies of granodiorites-granites in Southeast China have revealed a Mesozoic, northeast-trending high-potassium, low-T_{DM} magmatic zone (Shi-Hang zone, Gilder et al., 1996) that is cut by NS-striking Wanyangshan-Zhuguangshan granitic composites within the South China Block (Chen and Jahn, 1998) (Fig. 1A). The Mesozoic granodiorites-granites in the Shi-Hang zone are characterized by significantly high Sm (>8 ppm) and high Nd contents (>45 ppm) with relatively high $\varepsilon_{Nd}(t)$ values (–4 to –8). They are interpreted as a result of mantle upwelling along a "paleo-rift" (Gilder et al., 1996; Wang et al., 2003b; Li et al., 1999; Chen and Jahn, 1998).

[1]Corresponding author; email: liangxq@gig.ac.cn

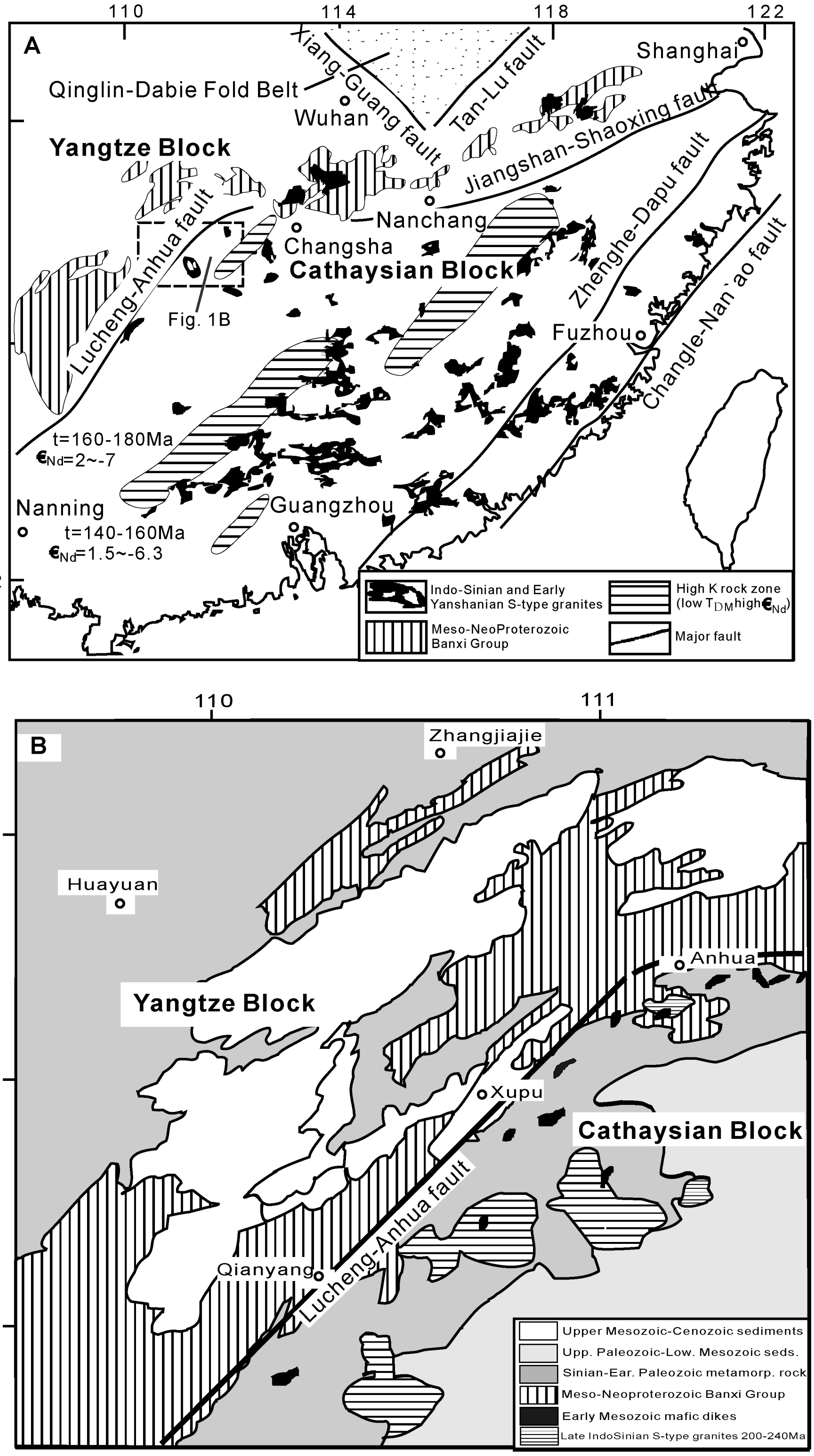

FIG. 1. (*See caption on facing page*)

FIG. 1. A. A simplified tectonic map of southern China, showing the distribution of Mesozoic high-K, high ε_{Nd} zones (after Chen and Jahn, 1998; Li et al., 1999; Li, 2000; Wang Y. J. et al., 2003b). B. Geologic map showing the distribution of the Mesozoic shoshonitic lamprophyres in the Anhua-Xupu area, Hunan Province, southern China. The boundary between the Yangtze and Cathysian blocks is defined by the occurrence of the Meso- and Neoproterozoic Banxi Group (Chen and Jahn, 1998).

In this paper, we report whole-rock major and trace elements and Sr-Nd isotope data for the Anhua-Xupu lamprophyres, K-rich mafic rocks emplaced along the western margin of the South China orogen. These rocks possess fine- to very fine grained porphyritic textures and homogeneous chemical compositions. Bulk-rock analyses are furthermore characterized by very enriched LILE, strongly enriched LREE, and relatively depleted HREE and HFSE. Age-corrected initial $^{87}Sr/^{86}Sr$ ratios span the narrow range of 0.721565–0.722292 and $\varepsilon_{Nd}(t)$ = –9.81 to –10.45. These new geochemical data allow study of the petrogenesis of those lamprophyres, and provide constraints on the tectonic evolution of South China in the Early Mesozoic.

Occurrence and Petrologic Features

The Anhua-Xupu lamprophyres, mainly plagiominettes occur as dikes. More than 60 dikes in the Xuefengshan Mountains are located in the Shibadu and Dongdiping areas of Anhua and Xupu counties, near the northeastern end of the Lucheng-Anhua fault (Fig. 1). Dikes are clearly the products of post-orogenic events, showing no evidence of deformation. They intruded the Cambrian and Ordovician limestones, as well as the Wangyun Late Triassic granite (U-Pb zircon age of 211 Ma; Fig. 1B) (HBGMR, 1988). In general, typical dikes are 0.6 m wide, but the maximum widths are up to 10 m. The longest known dike array has a strike length of 1.5 km in the Shibadu, Anhua district, Hunan Province. The dikes, whose country rocks experienced low-grade contact metamorphism, are branched and rejoined, controlled by the NW-trending subordinate structures of the NE-trending Jingxian-Xupu fault. They strike roughly N60°E and dip southeast.

The studied samples are relatively fresh and exhibit gray-yellow colors. Some lamprophyres (e.g., SH-1, 2 and 3) show typical porphyritic textures. The groundmass is very fine grained, typically glassy and consists mainly of plagioclase (An_{45}, 40–60%), biotite (35–40%), clinopyroxene (0–10%), K-feldspar (1–10%), and quartz (1–5%). Phenocrysts consist of phlogopite, clinopyroxene, amphibole and plagioclase. Phlogopite commonly shows flow textures. Moreover, the rocks generally underwent a low degree of alteration as a consequence of calcitization and sericitization. Some andesine crystals exhibit circular rims of potassium feldspar. The lamprophyres contain abundant accessory magnetite, ilmenite, limonite, chromite, zircon, rutile, apatite and monazite.

Whole rock K-Ar ages of about 207±3 Ma, determined by the Isotopic Laboratory of Guangzhou Institute of Geochemistry, Chinese Academy of Sciences, indicates a Late Triassic emplacement of the lamprophyre dikes. Alternatively, stratigraphic evidence suggest that the magma activity may have started in the Middle to Late Triassic (HBGMR, 1988).

Geochemical Characteristics

General classification

Major element analyses of the Anhua-Xupu lamprophyres are listed in Table 1. SiO_2 content varies from 47.20% to 52.62%, K_2O = 2.36–3.67%, K_2O + Na_2O = 4.33–6.41%, K_2O/Na_2O = 0.84–1.72, TiO_2 = 0.54–1.21%, and Al_2O_3 = 13.32–16.28%. The oxidation coefficient W [$Fe_2O_3/(Fe_2O_3$ + FeO)] ranges from 0.25 to 0.43. The chemical compositions of the lamprophyres are similar to that of K-alkali-basaltic rocks (Joplin, 1968; Morrison, 1980; Foley and Peccerillo, 1992; Duggan and Jaques, 1994; Muller and Groves, 1995).

The geochemical data presented in Table 1 show that all of the samples are rich in potassium. On a conventional Harker diagram of K_2O vs. SiO_2 (Fig. 2A), the samples define a rough trend between 50% and 62% of SiO_2 at high K_2O (generally >2.5 %), and lie almost totally within the shoshonite field defined by Peccerillo and Taylor (1976).

Applying the trace element classification (Fig. 2B) by Pearce (1982), the rocks studied plot well in the shoshonitic field. On the Zr/TiO_2-Nb/Y classification diagram by Winchester and Floyd (1976), all lamprophyres fall in the field of trachybasalt and trachyandesite (Fig. 2C). These indicate that the

TABLE 1. Major and Trace Element Data for the Shoshonitic Lamprophyres in the Anhua-Xupu Area, Southern China

Sample	SH-1	SH-2	SH-3	YP-4	D-3	D-5	D-8	D-12	X-1	X-2	X-3
					Major elements, wt.% [1]						
SiO_2	48.52	48.14	48.3	51.26	49.06	49.72	49.28	52.62	49.28	47.2	48.24
TiO_2	0.93	0.97	0.88	0.76	0.94	1.21	0.91	0.54	0.94	0.92	0.93
Al_2O_3	13.66	13.52	13.65	14.03	14.63	14.67	16.28	14.86	13.49	13.32	13.41
Fe_2O_3	2.35	1.86	1.83	2.63	2.79	2.43	2.92	3.6	1.97	3.25	2.61
FeO	5.38	5.47	5.5	4.78	5.62	5.08	4.9	4.18	5.38	4.36	4.87
MnO	0.12	0.08	0.06	0.15	0.4	0.15	0.28	0.84	0.08	0.09	0.05
MgO	10.64	9.74	9.83	7.7	10.43	8.35	9.41	8.55	11.62	9.61	10.62
CaO	6.88	8.26	8.26	7.04	5.76	7.17	6.04	5.86	6.08	6.01	6.05
Na_2O	3.49	3.12	2.98	2.22	2.13	2.16	2.67	3.21	1.97	1.87	1.62
K_2O	2.92	2.7	2.72	2.36	3.67	3.62	3.25	2.83	2.6	3.41	2.71
P_2O_5	0.50	0.51	0.47	0.28	0.8	0.87	0.46	0.21	0.45	0.50	0.25
LOI	4.36	5.42	5.34	6.26	3.86	4.3	3.39	2.7	6.06	7.59	8.58
					CIPW norm						
Q	0	0	0	3.69	0	0	0	0	0	0	0
or	16.29	13.11	13.22	14.98	22.33	22.44	19.94	17.2	16.45	22.28	17.55
ab	29.57	27.76	26.54	20.13	18.51	19.13	23.41	27.88	17.81	17.46	14.99
an	14.54	17.57	18.52	22.86	20.02	20.53	23.64	18.23	21.65	19.7	23.28
ne	0.78	0.03	0	0	0	0	0	0	0	0	0
di	11.83	17.98	17.39	10.27	3.62	9.08	3.51	8.28	6.21	7.91	6.32
hy	0	0	2.17	21.78	15.71	13.98	6.2	16.49	25.39	17.31	29.41
ol	20.41	17.59	16.52	0	12.01	6.74	15.88	5.04	6.48	7.02	1.77
mt	3.58	2.85	2.8	4.09	4.16	3.69	4.39	5.36	3.06	5.2	4.14
il	1.86	1.94	1.76	1.55	1.84	2.41	1.79	1.05	1.91	1.93	1.93
ap	1.15	1.17	1.08	0.66	1.8	1.99	1.04	0.47	1.05	1.21	0.6
					Trace elements, ppm[2]						
Ni	267.95	223.53	272.49	256.48	139.06	182.25					
Cr	533.46	436.68	546.86	513.76	248.97	358.56					

Cs	4.23	5.47	4.40	5.73	4.94	4.79
Rb	178.53	178.82	152.48	92.63	165.65	141.21
Ba	2598.71	2537.12	2408.70	8034.30	2472.91	4347.24
Th	80.11	87.72	81.81	32.49	84.77	64.80
U	7.55	8.18	7.60	3.02		6.06
Nb	16.61	17.94	16.77	8.27	17.35	13.88
Ta	0.94	1.02	0.97	0.51	0.99	0.81
La	114.64	147.80	113.84	93.24	130.82	107.24
Ce	277.05	301.01	275.96	196.60	288.48	249.87
Pr	27.86	29.96	30.03	18.72	29.99	25.54
Sr	262.98	316.34	316.16	490.54	316.25	356.56
P	24.14	24.72	22.76	13.65	23.74	20.18
Nd	94.38	101.06	94.56	81.18	97.81	83.37
Zr	350.51	452.60	427.61	234.83	440.11	337.65
Hf	10.31	11.30	10.61	6.60	10.95	9.17
Sm	11.62	12.59	11.41	10.82	12.00	11.28
Eu	2.06	2.25	2.06	1.25	2.15	1.79
Dy	4.14	4.51	4.16	3.66	4.33	3.98
Y	21.75	23.49	22.00	20.06	22.74	21.27
Yb	2.02	2.20	2.03	1.84	2.12	1.96
Tb	0.80	0.87	0.78	0.66	0.83	0.75
Lu	0.29	0.33	0.31	0.27	0.32	0.29

[1]Major oxide contents were analyzed at the Hubei Institute of Geology and Mineral Resource, Chinese Ministry of Land and Resources, by wavelength X-ray fluorescence spectrometery, with analytical errors better than 2%. FeO content in sample is solely analyzed by a wet chemical method.

[2]Trace element analysis was performed at the Guangzhou Institute of Geochemistry, Chinese Academy of Sciences, by inductively coupled plasma mass spectrometry (ICP-MS). The detailed analytical procedure is described in Liu et al. (1996). Reproductivity is better than 95%, with general analytical error less than 5%. Mg # = 100*Mg/(Mg + Fe^{2+}); w = Fe_2O_3/FeO + Fe_2O_3; Fe^T = 0.0898 Fe_2O_3 + FeO. Chondrite data from Taylor and McLenann (1985). Primitive mantle from Sun and McDonough (1989).

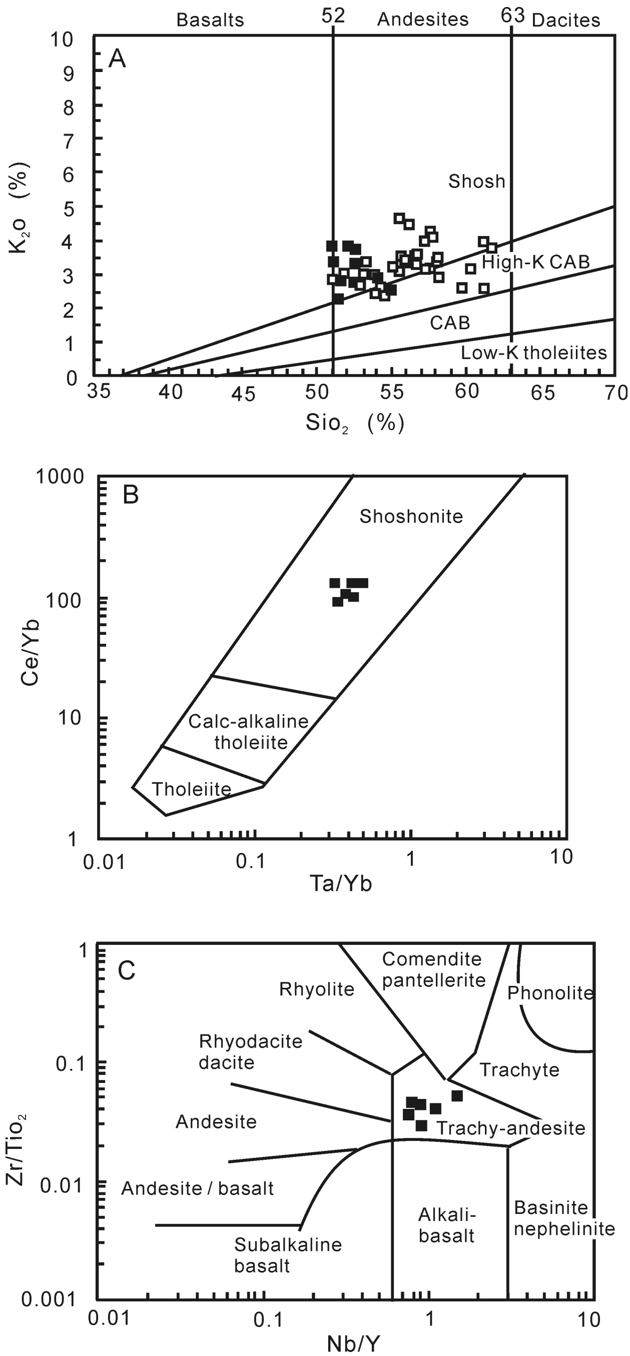

FIG. 2. Classification diagram for the Anhua-Xupu lamprophyres. A. K_2O vs. SiO_2 (after Peccerillo and Taylor, 1976; ultrapotassic as defined by Foley et al., 1987). B. Ce/Yb vs. Ta/Yb (Pearce, 1982). C. Zr/TiO_2–Nb/Y (Winchester and Floyd, 1976). Solid squares represent data used in this study; open squares represent data of the 413 Geological Team, Hunan Bureau of Geology and Mineral Resources (1982, unpubl. data).

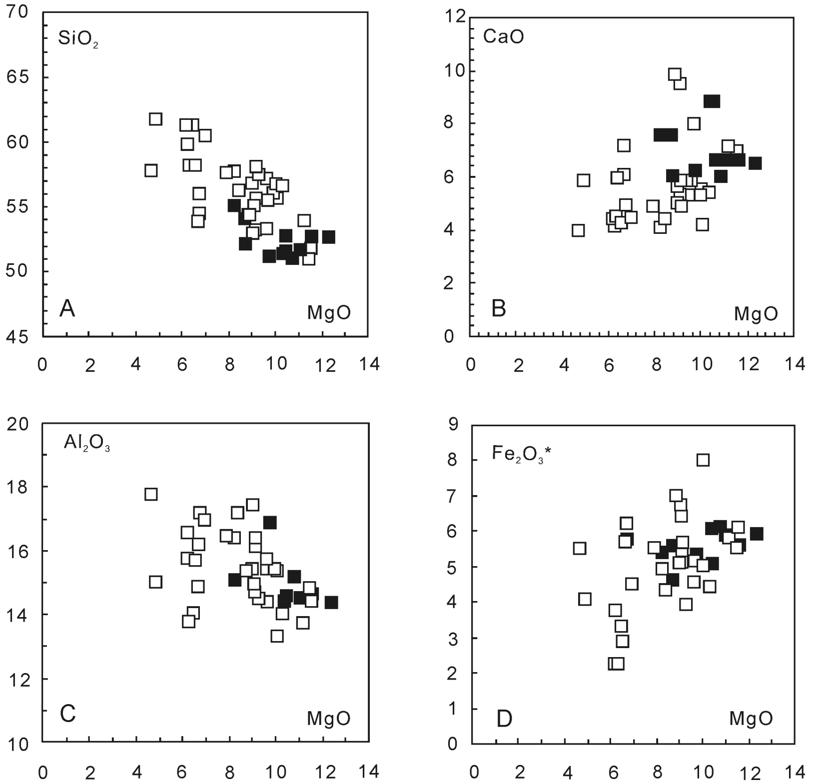

FIG. 3. Selected major element–MgO variation diagrams illustrating the broad compositional range of the Anhua-Xupu lamprophyres, which extends back to fairly magnesian compositions (MgO 8–11%). Solid squares represent data from this study; open squares represent data of the 413 Geological Team, Hunan Bureau of Geology and Mineral Resources (1982, unpubl. data).

Anhua-Xupu lamprophyres generally belong to the high-potassium rock series from basaltic to trachytic composition.

Despite their high K_2O, they are not ultra-potassic, having K_2O/Na_2O ratios between 0.5 and 2.0 (Table 1), again, within the field of shoshonitic magmas. The Mg ratios [=100*Mg/(Mg + Fe^{2+}) atomic] ranges from 74 to 80, and SiO_2 and Al_2O_3 decrease, whereas CaO and Fe_2O_3 (which has an inflection at 5% MgO) increase, with increasing MgO (Fig. 3). TiO_2 (not plotted) shows an inflected trend and the absolute abundances of Al_2O_3 and TiO_2 are low, with averages of 13–16% and 0.5–1.5%, respectively. K_2O and Na_2O have related constant abundances though K_2O is always slightly greater than Na_2O ($K_2O/Na_2O \leq 2$). The rocks broadly lie at the projected end of trends defined by mafic-dominant compositions, being highly depleted in TiO_2 and CaO, where K_2O and Na_2O abundances remain similar to those of the mafic lavas.

CIPW norms calculated on a volatile-free basis indicate subalkaline compositions which are either *qz-hy* or *ol-hy* normative. Most lamprophyres straddle the silica-saturation boundary, and rarely have normative *ne* or qz but are strongly *ol* normative (Table 1).

Trace elements

Twenty-five trace elements have been determined (Table 1). Globally, all lamprophyres have similar REE concentration levels and are highly enriched in incompatible elements (for example, La ranges from 90 to 115 ppm). In the REE variation diagram (Fig. 4A), REE patterns of the studied samples are similar in shape but differ in total REE contents (ΣREE = 395–612 ppm). The patterns show

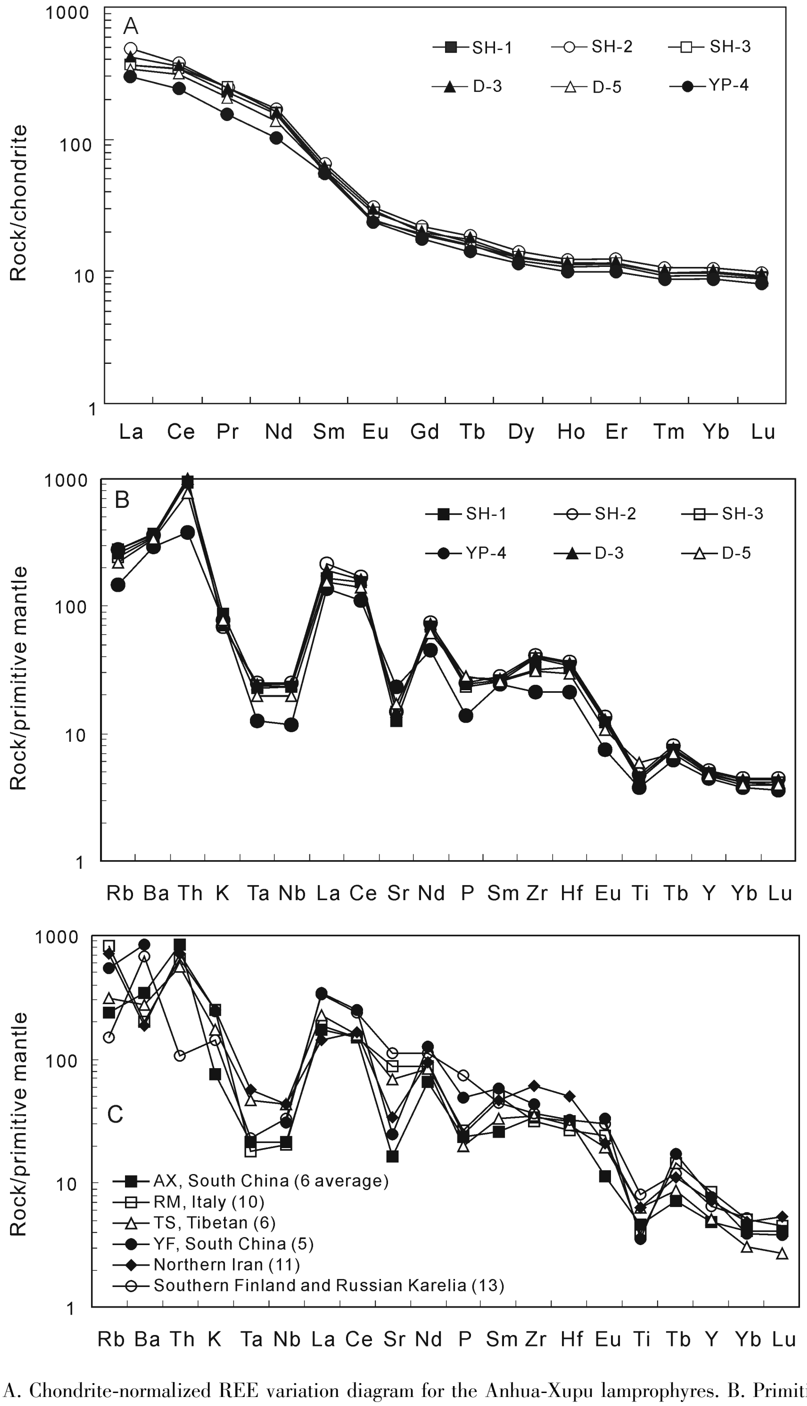

FIG. 4. A. Chondrite-normalized REE variation diagram for the Anhua-Xupu lamprophyres. B. Primitive mantle–normalized variation diagram for the Anhua-Xupu lamprophyres. C. Primitive mantle–normalized variation diagram for the K-rich rocks from central Italy (Battistini et al., 1998), southern Finland (Eklund et al., 1998), the Tibetan Plateau (Turner et al., 1996; Williams et al., 2001, 2004; Ding et al., 2003), and the Wuyi Mountains, southern China (Wang Q. et al., 2003). Chondrite and primitive mantle normalizing values are from Sun and McDonough (1989).

strongly fractionated LREE (La_N/Sm_N = 5.4–7.4, normalized to the chondritic values from Sun and McDonough, 1989), high LREE/HREE ratios (La_N/Yb_N = 34–46), and slight or no Eu negative anomalies (Eu/Eu* = 0.64–0.86).

The primitive mantle–normalized patterns of incompatible elements (Fig. 4B) show a characteristic depletion in HFSE (Ti, P, Nb, Ta) relative to LILE (Rb, K, Ba,Th). A strong negative spike at Sr (Fig. 4B) is another relevant feature of the primitive mantle–normalized patterns.

The trace element patterns of the Anhua-Xupu shoshonitic lamprophyres (AX) are identical to those of melilitites in Roman Magmatic Province, Italy (RM) (Battistini et al., 2001) and the Tibetan shoshonitic volcanism (TS) (Turner et al., 1996; Ding et al., 2003; Williams et al., 2001, 2004), both for the most incompatible elements (Rb, Ba, Th, U) and for the REE and HFSE. The Nb and Ta anomalies show similar features (lowering as much as 50 times the primitive mantle values for TS, 20 for RM, and 25 for AX). P and Ti anomalies indicate the same characteristic and Sr displays a strong negative anomaly in the Anhua-Xupu lamprophyres (Fig. 4C). A similar pattern occurs in the shoshonitic rocks from Central Alborz, northern Iran (Fig. 4C; Mehdizadeh et al., 2002), southern Finland and Russian Karelia (Fig. 4C; Eklund et al., 1998), Black Forest, Germany (Hegner et al., 1998), and the Yangfang aegiriteaugite syenite from Wuyi Mountains of South China (Fig. 4C, Wang Q. et al., 2003).

Sr and Nd isotopes

Measured, age-corrected $^{87}Sr/^{86}Sr$ and $^{143}Nd/^{144}Nd$ ratios are listed in Table 2. The initial $^{87}Sr/^{86}Sr$ and $^{143}Nd/^{144}Nd$ ratios vary within narrow ranges of 0.721565–0.722292 and 0.511836–0.511869, respectively. The latter corresponds to $\varepsilon_{Nd}(t)$ = –9.81 to –10.45. As illustrated in Figure 5, all the studied samples are plotted in the enriched mantle quadrant. They are isotopically indistinguishable from Early Mesozoic (250–165 Ma) granitoids (Gilder et al., 1996) and the lower/middle crust (LC/MC) in the South China Block (Guo et al., 1997b; Li, 1990), but are distinct from Early Mesozoic mafic rocks, potassium-rich diorites-granodiorites, and the Kongling TTG Group in the South China Block (Chen and Jahn, 1998; Shen et al., 1998; Guo et al., 1997b; Li, 1990; Gao et al., 1999; Wang Y. Q. et al., 2003a, 2003b; Li et al., 2004). The Nd model ages relative to depleted mantle range between 1.30 and 1.37 Ga for the Anhua-Xupu lamprophyres (Table 2).

Discussion

Petrogenesis of shoshonitic magmas

The trace and rare-earth elements and isotopes of the studied shoshonitic lamprophyres are all relatively homogeneous. The maximum Ni content of the studied rocks (e.g., SH-3: 272 ppm; SH-1: 267 ppm; D-5: 282 ppm) is quite low in comparison to the common mantle magmas with similar Mg numbers (Frey et al., 1978; Wilkinson and Le Maitre, 1987; Wang Y. J., et al., 2003a, 2003b), whereas the Cr contents of the lamprophyres (450–570 ppm) fall in the range expected for primitive mantle magmas (500–600 ppm). It is worthy of note that the lamprophyres have been recognized as the most primitive rock types. Nb/Ta ratios (17.08–17.67) and Zr/Hf ratios (35.58–40.31) are also similar to the ratios for primary mantle (17.5 ± 2.0 and 36.27 ± 2.0, respectively), but are much higher than the ratios for continental crust (11 and 33; Taylor and McLenann, 1985; Weaver, 1991), demonstrating that crustal hybridization played only a small role in the magmatic evolution. The aphyric or poorly porphyritic texture of some samples (e.g., YP-4, D-3, D-5) excludes the possibility that such values were produced by mafic mineral accumulation. This not only supports a mantle provenance for the parental magmas of the potassic suites, but also limits the role of the continental crust in determining the geochemical characteristics of these liquids. It is thus clear that the geochemical characteristics of the lamprophyre reflect the nature of the mantle source region.

The Anhua-Xupu shoshonitic lamprophyres have lower incompatible-element contents than potassic or ultrapotassic rocks from Roman, Italy (Rogers et al., 1985; Sun and McDonough, 1989; Battistini et al., 2001), southern Finland (Eklund et al., 1998), and the Tibetan Plateau (Turner et al., 1996), but display a similar distribution pattern of incompatible elements with a high ratio of large-ion-lithophile elements versus high-field-strength elements and strong negative anomalies of Ta, Nb, and Ti. A similar pattern occurs in the leucite tephrite from the Aeolian arc, in the rocks from Radicofani and Cimina (Peccerillo, 1985), and in the Yangfang aegirine-augite syenite from the Wuyi Mountains of South China (Fig. 4C; Wang Q. et al., 2003). High LIL/HFS ratios (e.g., La/Nb = 5.17–

TABLE 2. Rb-Sr and Sm-Nd Isotopic Data for the Shoshonitic Lamprophyres (t = 207 Ma) in the Anhua-Xupu area, Hunan Province, China

Sample	Rb, ppm[1]	Sr, ppm[1]	$^{87}Rb/^{86}Sr$	$^{87}Sr/^{86}Sr \pm 2\sigma$[2]	Sm, ppm[1]	Nd, ppm[1]	$^{147}Sm/^{144}Nd$	$^{143}Nd/^{144}Nd \pm 2\sigma$[2]	$^{87}Sr/^{86}Sr(i)$	$^{143}Nd/^{144}Nd(i)$	$\epsilon_{Nd}(t)$	T_{DM}(Ga)
SH-1	178.53	262.98	1.968	0.722144 ± 11	11.62	94.38	0.074463	0.511937 ± 8	0.721565	0.511836	–10.45	1.33
SH-2	178.82	316.34	1.639	0.722774 ± 14	12.59	101.06	0.075346	0.511971 ± 8	0.722292	0.511869	–9.81	1.30
SH-3	152.48	316.16	1.398	0.722406 ± 9	11.41	94.56	0.072978	0.511948 ± 6	0.721995	0.511849	–10.20	1.31
YP-4	92.63	490.54	0.547	0.722432 ± 12	10.82	81.18	0.080610	0.511973 ± 8	0.722271	0.511864	–9.91	1.35
D-3	165.65	316.25	1.519	0.722590 ± 12	12.00	97.81	0.074201	0.511960 ± 6	0.722144	0.511859	–10.00	1.30
D-5	141.21	356.56	1.148	0.722327 ± 16	11.28	83.37	0.081830	0.511966 ± 9	0.721990	0.511855	–10.08	1.37

[1]The Rb, Sr, Sm, and Nd abundances were measured by ICP-MS at the Guangzhou Institute of Geochemistry, Chinese Academy of Sciences. $^{87}Rb/^{86}Sr$ and $^{147}Sm/^{144}Nd$ ratios were calculated using Rb, Sr, Sm, and Nd abundances measured by ICP-MS.

[2]Sr and Nd isotope ratios were measured by a VG 354 mass spectrometer at the Institute of Geology and Geophysics, Chinese Academy of Sciences. The ratios were normalized to $^{86}Sr/^{88}Sr = 0.1194$ and $^{146}Nd/^{144}Nd = 0.7219$, respectively. The whole procedure blanks are lower than 5×10^{-10} g for Sr and 5×10^{-11}g for Nd. Thirteen analyses of standard La Jolla gave $^{143}Nd/^{144}Nd = 0.511962 \pm 10$, and two analyses of BCR-1 gave $^{143}Nd/^{144}Nd$ ratios of 0.512626 ± 9. Six analyses of NBS 987 gave $^{87}Sr/^{86}Sr = 0.710265 \pm 12$, and two analyses of NBS607 gave $^{87}Sr/^{86}Sr = 1.20032 \pm 3$ (1 s.d.) (Wang Y. J. et al., 2003a). Initial ratios were calculated using 207Ma. ϵ_{Nd} (t) calculation parameter: $(^{143}Nd/^{144}Nd)_{CHER}(0) = 0.512638$, $(^{147}Sm/^{144}Nd)_{CHER} = 0.1967$.

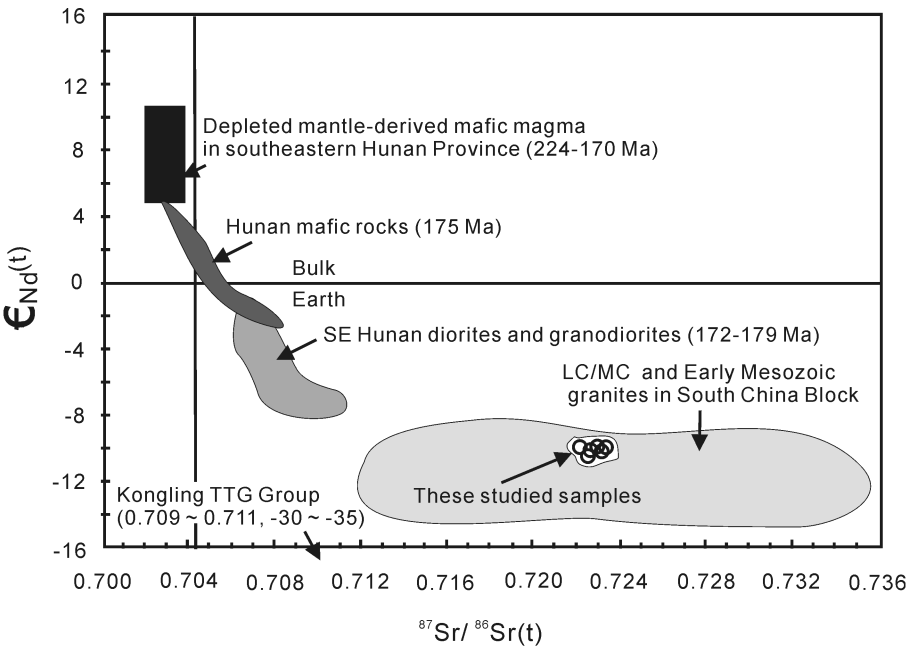

FIG. 5. $^{87}Sr/^{86}Sr(t)$ vs. $\varepsilon_{Nd}(t)$ diagram for the Anhua-Xupu shoshonitic lamprophyres in Hunan Province, southern China (McCulloch et al., 1983), showing that these samples are isotopically different from the neighboring Early Mesozoic (175 Ma) potassium-rich diorites-granodiorites and mafic rocks. Data sources: LC/MC in the South China Block (Li, 1990; Guo et al., 1997a, 1997b); Early Mesozoic S-type granites (Chen and Jahn, 1998; Shen et al., 1998; Gilder et al., 1996); lower crust of the Yangtze Block represented by Kongling TTG rocks (Gao et al., 1999); depleted mantle-derived mafic magma in Hunan Province (224–170 Ma) (Guo et al., 1997b; Zhao et al., 1998); Early Mesozoic (175 Ma) mafic rocks (Wang Y. J. et al., 2003b; Li et al., 2004); Early Mesozoic (175 Ma) diorites and granodiorites (Wang Y. J. et al., 2003a).

8.24, Ba/Nb = 141.41–439.76) and negative anomalies of Ta, Nb, and Ti are typical of all island-arc rocks (e.g., Perfit et al., 1980; Peccerillo, 1985, 1998; Eklund et al., 1998; Mehdizadeh et al., 2002).

In the Sr and Nd isotopic diagram, the Anhua-Xupu rocks plot on a hyperbolic curve linking depleted mantle (DM) with lower and middle crustal rocks (Fig. 5). As a consequence, these magmas have commonly been interpreted as the result of mixing processes involving mantle and continental crust rocks of variable compositions. Mixing achieved by means of crustal assimilation has been proposed in the past by some authors (e.g., Vollmer, 1977; Wang Y. J. et al., 2003a), but was rejected as a major petrogenetic process by Holm and Munksgaard (1982) and Conticelli and Peccerillo (1992), who considered the enriched isotopic compositions as well as the peculiar geochemical features of the high-potassium series and potassium-series rocks as primary features inherited from the mantle.

Assuming that a crustal component necessarily must be involved, the only mechanism capable of adding a crustal component directly to the mantle source region of the magmas is subduction: two-component mixing processes related to subduction mechanisms would easily account for the apparent "orogenic" signature of these rocks, i.e., low concentrations of Nb and TiO_2 and high LILE/HFSE ratios. These Anhua-Xupu shoshonitic lamprophyres have restricted Sr-Nd isotope ratios and pronounced Nb-Ta negative anomalies of typical arc signature. Hence, their refractory mantle source domain, residing most likely in the continental lithospheric mantle, must have been metasomatized by subduction-related enrichment before being partially melted to produce the high-Mg, potassium-rich magma. This subduction-related metasomatism event is not well understood, but possibly occurred during the Middle–Late Proterozoic orogeny (Zhou et al., 1989; Zhou and Zhu, 1993). Information

TABLE 3. Comparison of Ti, Zr, and Nb Contents between the Studied Lamprophyre and Some Arc Shoshonitic Lamprophyres

	Anhua-Xupu shoshonitic lamprophyres	Oceanic subduction arc		Continental rift alkalic basalt
		Shoshonite	Andesite	
TiO_2, %	0.76–1.17	0.85	0.58	2.2
Zr, 10^{-6}	234.83–582.35	150	90	800
Nb, 10^{-6}	8.27–33.76	5–7		50–90
Data source	This paper	TiO_2, Zr (Condie, 1982), Nb (Xu, 1988)		TiO_2, Zr (Condie, 1982), Nb (Zhi, 1990)

about the possible source ages of the Anhua-Xupu lamprophyres can be obtained using Nd-model ages. Based on depleted mantle Nd-model ages (1.3–1.37 Ga; Table 2), the precursory enrichment of the mantle source may have taken place long before the magmatic event.

The shoshonitic lamprophyres have a wide range of CaO and K_2O. The K_2O appears to correlate positively with Al_2O_3, TiO_2, Fe_2O_3, and LREE, but negatively with CaO, Sr, and Ba, implying a phlogopite- and clinopyroxene-bearing lithospheric mantle (Nelson et al., 1986; Foley, 1992a, 1992b). Alternative interpretations involving significant crustal contamination to the asthenosphere-derived magmas are not favored because of their very high MgO contents (8–11%) and low Nb/La ratios (0.18–0.25), which are much lower than continental crust values (averaging 0.5–0.8; Rudnick and Fountain, 1995). A detailed geochemical and isotopic study is needed to provide further constraints on the mantle source of these high-K shoshonitic lamprophyres.

Tectonic implications

Studies indicate that shoshonitic lamprophyres are, as a rule, derived from metasomatic mantle enriched in potassium and LILE, related to subduction, occurring in original and late-stage oceanic arcs, continental arcs and post-collisional arcs, and rarely occurring in intraplate rifts or divergent continental margins (Morrison, 1980; Peccerillo, 1985; Rogers et al., 1987; Foley and Peccerillo, 1992; Duggan and Jaques, 1994; Muller and Groves, 1995; Turner et al., 1996).

Shoshonitic rocks formed in the oceanic within-plate settings, such as Gough and Tristan da Cunha Islands (Weaver, 1991), show typical OIB-type geochemical characters, whereas shoshonitic rocks formed in continental within-plate settings may have arc-type geochemical features, such as Colorado (Leat et al., 1988), Borneo (Central Kalimantan, Indonesia; Bergman et al., 1988) and the Lachlan Fold Belt (southeastern Australia; Wyborn, 1992), or OIB-type features, such as Virunga Province (East Africa Rift; Rogers et al., 19988).

Within-plate potassic magma commonly is generated during asthenosphere upwelling and thinning of the lithosphere. LILE enrichment within the lithospheric mantle may result from metasomatism associated with the underplating of plume-induced magma, or the long-term heterogeneity of the lithosphere. Nevertheless, potassic magma is generated by very low (?) degrees of partial melting of a phlogopite-bearing lithospheric mantle (Nelson et al., 1986). However, what is the tectonic setting and the dynamic significance of the Early Mesozoic shoshonitic lamprophyres occurring in the Anhua-Xupu area, South China?

Comparison of Ti-group elements between the Anhua-Xupu lamprophyres and arc shoshonitic lamprophyres related to oceanic subduction (Table 3) demonstrates that they are greatly different. TiO_2, Zr, and Nb contents of the Anhua-Xupu lamprophyres are higher than those of arc shoshonitic lamprophyres and lie between these of arc shoshonitic lamprophyres and continental rift alkalic basalts. This indicates that the Anhua-Xupu lamprophyres have features of both arc volcanic rocks and within-plate volcanic rocks, in accordance with the dual features of an intracontinental orogenic belt (Deng et al., 1996).

In Al_2O_3 versus TiO_2, TiO_2/Al_2O_3 versus Zr/Al_2O_3, and Zr/TiO_2 versus Ce/P_2O_5 diagrams (Figs. 6A–6C; (Muller et al., 1992; Muller and Groves, 1993), the samples of the shoshonitic lamprophyres lie mostly in the continental arc field, and rarely in the within-plate field. However, in the Y versus Zr

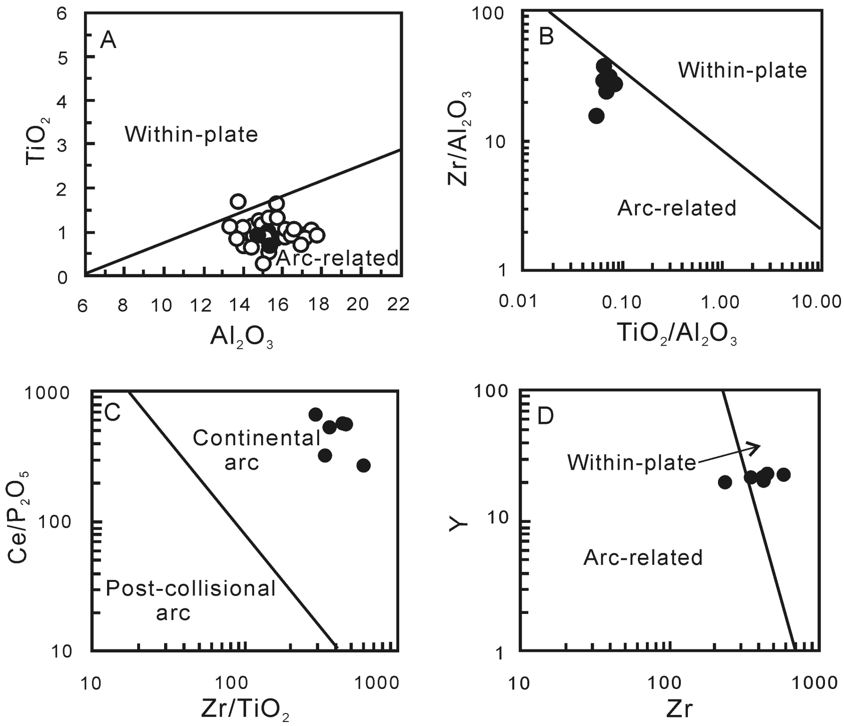

FIG. 6. Discrimination diagrams for tectonic setting of the shoshonite lamprophyre (Muller et al., 1992; Muller and Groves, 1993). A. Al_2O_3 versus TiO_2. B. TiO_2/Al_2O_3 versus Zr/Al_2O_3. C. Zr/TiO_2 versus Ce/P_2O_5. D. Zr versus Y. Black circles represent data from this study; open circles represent data of the 413 Geological Team, Hunan Bureau of Geology and Mineral Resources (1982, unpubl. data).

diagram (Fig. 6D), they plot in the within-plate field. Obviously, their tectonic setting is related to both subduction and within-plate. The former may reflect the character of the origin of the mantle source regions; the latter may be a tectonic setting of the petrogenesis of the Anhua-Xupu shoshonitic lamprophyres. Although they show Nb and Ta depletions (Fig. 4B), a feature that is typically related to arc magma, they are not formed in an arc setting. Their Nb and Ta depletions are possibly related to partial melting of the mantle source metasomatized by fluids released from the paleo-subduction zone. Therefore, the existence of Early Mesozoic Anhua-Xupu shoshonitic lamprophyres suggests that the Early Indosinian extension event probably was active in the Anhua-Xupu area of southern China.

The Mesozoic tectonic evolution of the South China Block has been debated for the past two decades, and no general agreement has been reached up to now. Two distinct hypotheses have been postulated. One suggests that the tectonic evolution was related to westward subduction of a Mesozoic Pacific plate, or due to closure of an oceanic basin in the interior of the South China Block (Hsü et al., 1988, 1990; Faure et al., 1996; Zhou and Li, 2000). However, paleomagnetic evidence has demonstrated that the west-dipping subduction of a Pacific plate occurred no earlier than 125 Ma (Engebretson et al., 1985). This tectonic model has also been challenged by the absence of contemporaneous ophiolite suites, oceanic basins, and island-arc magmatism. The second hypothesis advocates that continental rifting and lithospheric extension was the dominant mechanism since the Early Mesozoic, probably even Paleozoic time (Rowley et al., 1989; Gilder et al., 1996; Chen and Jahn, 1998; Zhao et al., 1998; Li, 2000; Li et al., 2003; Wang Q. et al., 2003; Wang Y. J. et al., 2003b).

The NE-trending potassium-rich calc-alkaline diorites-granodiorites in the interior of the South China Block (Fig. 1A) have arc-type trace element signatures and relatively high $^{87}Sr/^{86}Sr$ and lower ε_{Nd}. They mainly originated from enriched lithospheric mantle that was partially melted due to a raised geotherm caused by lithospheric thinning (Gilder et al., 1996; Li et al., 2000, 2003, 2004; Wang Y. J. et al., 2003a). We therefore suggest that the Anhua-Xupu shoshonitic lamprophyres also probably were derived by the partial melting of a clinopyroxene- and phlogopite-rich mantle source under an extension setting.

Taking into account the occurrence of the Early Triassic intra-continental orogenic event (HBGMR, 1988; Rowley et al., 1989), it is likely that the lithospheric extension commenced from the Middle–Late Triassic in response to post-Indosinian orogenic collapse (Zhao et al., 1998; Wang Q. et al., 2003; Li et al., 2003), and subsequently dominated the tectonic development of the South China Block interior until ca. 130 Ma (Li, 2000). The lithospheric extension hypothesis is also supported by evidence of doming of the contemporaneous metamorphic core complexes in Wugongshan, Lushan, Mofushan, and Jiu lingshan (Faure et al., 1996; Shu et al., 1998; Lin et al., 2000, 2001). Shui (1987) suggested that Cathaysia started to extend after the Caledonian, and lasted through the Indosinian to the Yanshanian. Faure et al. (1996) and Shu et al. (1998) considered that the dome extension structure in the Wugongshan area of Jiangxi Province started in the Triassic (225–230 Ma). Carter et al. (2001) thought that the Indosinian orogeny in Southeast Asia was triggered by an oblique convergence of the Sibumasu Block to the Indosinian–South China Block at 258–243 Ma. High-temperature metamorphism during the Indosinian orogeny terminated at 243 ± 5 Ma with a regional rapid exhumation. The cause of the rapid exhumation may be linked to changes in the regional stress field between initial stages of oblique convergence (transpression) and the clockwise rotation of the fully accreted Sibumasu–Indosinian–South China terranes (transtension). Furthermore, the Late Triassic–Cretaceous extensional basins, such as the Shiwandashan basin in southeastern Guangxi (Gilder et al., 1996), were mostly developed on the Paleozoic to Middle Triassic basement that was ubiquitously folded by the Indosinian orogeny (Li, 1998). Thus, the rifting and extension are likely to have commenced in the Late Triassic–Early Jurassic. The petrogenesis of the Anhua-Xupu shoshonitic lamprophyres is probably related to these Late Triassic–Early Jurassic extensional events. The dating result provides a new insight for further understanding of the "Indosinian orogeny" in southern China.

Conclusions

The Anhua-Xupu shoshonitic lamprophyres are characterized by high $K_2O + Na_2O$ contents (4.33–6.41%), a high K_2O/Na_2O ratio (0.84–1.72), and low TiO_2 contents (0.54–1.21%). They display the typical geochemical and isotopic signatures of the island-arc rocks or K-rich magmas, i.e., low TiO_2, low K_2O/Al_2O_3, high LILE/HFSE ratios, highly radiogenic $^{87}Sr/^{86}Sr$ and unradiogenic $^{143}Nd/^{144}Nd$ (initial $^{87}Sr/^{86}Sr$ = 0.721565–0.722292 and $\varepsilon_{Nd}(t)$ = –9.81 to –10.45), varying in a narrow range. Geochemical and isotopic signatures shown by the Anhua-Xupu primary magmas require a clinopyroxene + phlogopite–rich mantle source; in particular, partial melting of a veined lithospheric mantle can account for the occurrence of different primary magmas characterized by relatively constant Sr- and Nd-isotopic compositions. Depleted mantle Nd-model ages (1.30–1.37 Ga) suggest that the mantle enrichment may have been a reflection of Proterozoic subduction between the Yangtze and Cathaysian blocks. Judging from the regional tectonic evolution, it is reasonable to conclude that formation of these shoshonitic lamprophyres is related to Early Mesozoic post-collisional intra-lithospheric thinning.

Acknowledgments

We thank Senior Academician G. D. Chen and Prof. X. Y. Yang for guidance of the paper and field investigation, and Prof. F. Wang and D. L. Guo for assistance during the field work. We especially thank Prof. S. Z. Chen, from Geomatrix Consultants, Inc., California, formerly at Carleton University and Ottawa-Carleton Geoscience Center, Canada, who read an earlier version of this manuscript and offered many helpful and constructive suggestions. This work was co-supported by the National Natural Science Foundation of China (40334039 and 40272092), Chinese Academy of Sciences (KZCX2-102), China Postdoctoral Science Foundation (200333418), and Hunan Natural Science Foundation (2001).

REFERENCES

Battistini, G. D., Montanini, A., Vernia, L., Bargossi, G. M., and Castorina, F., 1998, Petrology and geochemistry of ultrapotassic rocks from the Montefiascone Volcanic Complex (central Italy): Magmatic evolution and petrogenesis: Lithos, v. 43, p. 169–195.

Battistini, G. D., Montanini, A., Vernia, L., Venturelli, G., and Tonarini, S., 2001, Petrology of melilite-bearing rocks from the Montefiascone Volcanic Complex, Roman Magmatic Province: New insights into the ultrapotassic volcanism of Central Italy: Lithos, v. 59, p. 1–24.

Bergman, S. C., Dunn, D. P., and Krol, L. G., 1988. Rock and mineral chemistry of Linhaisai minette and the origin of Borneo diamonds, Central Kalimantan, Indonesia: Canadian Mineralogist, v. 26, p. 23–44.

Carter, A., Roques, D., Bristow, C., and Kinny, P., 2001, Understanding Mesozoic accretion in Southeast Asia: Significance of Triassic thermotectonism (Indosinian orogen) in Vietnam: Geology, v. 29, p. 211–214.

Chen, H. H., Sun, S., Li, J. L, and Wang, Q. C, 1993, Apreliminary study on tectonics of the Xuefeng Mountains, western Hunan: Scientia Geologica Sinica, v. 28, p. 201–210 (in Chinese with English summary).

Chen, J. F., and Jahn, B. M., 1998, Crustal evolution of southeastern China, Nd and Sr isotopic evolution: Tectonophysics, v. 284, p. 101–133.

Condie, K. C., 1982, Plate tectonics and crustal evolution: London, UK, Pergamon Press, 265 p.

Conticelli, S., and Peccerillo, A, 1992, Petrology and geochemistry of potassic and ultrapotassic volcanism in central Italy: Petrogenesis and inferences on the evolution of the mantle sources: Lithos, v. 28, p. 221–240.

Deng, J. F., Zhao, H. L., Mo, X. X., Wu, Z. X., and Luo, Z. H., 1996, Continental roots-plume tectonics of China—key to continental dynamics: Beijing, Geological Publishing House, 110 p. (in Chinese with English summary).

Ding, L., Kapp, P., Zhong, D. L., and Deng, W. M., 2003, Cenozoic volcanism in Tibet: Evidence for a transition from oceanic to continental subduction: Journal of Petrology, v. 44, p. 1833–1865.

Duggan, M. B., and Jaques, A. L., 1994, Proterozoic shoshonitic lamprophyres from Tennant Creek, *in* Freeman, M. J., ed, Geoscience Australia: Sydney, Australia, Geological Society of Australia, p. 1–87.

Eklund, O., Konopelko, D., Rutanen, H, Frojdo, S., and Shebanov, A. D., 1998, 1.8 Ga Svecofennian post-collisional shoshonitic magmatism in the Fennoscandian shield: Lithos, v. 45, p. 87–108.

Engebretson, D. C., Cox, A., and Gordon, R. G., 1985, Relative motions between oceanic and continental plates in the Pacific basins: Geological Society of America Special Paper, v. 206, p. 1–59.

Faure, M., Sun, Y., Shu, L., Monie, P., and Charvet, J., 1996, Extensional tectonics with a subduction-type orogen: The case study of the Wugongshan dome (Jiangxi Province, SE China): Tectonophysics, v. 263, p. 77–108.

Foley, S., 1992a, Petrological characterization of the source components of potassic magmas: Geochemical and experimental constraints: Lithos, v. 28, p. 187–204.

Foley, S., 1992b, Vein-plus-wall-rock melting mechanism in the lithosphere and the origin of potassic alkaline magmas: Lithos, v. 28, p. 435–453.

Foley, S. F., Enturelli, G., Green, D. H., and Toscani, L., 1987, The ultrapotassic rocks, characteristics, classification and constraints for petrogenetic models: Earth Science Reviews, v. 24, p. 81–134.

Foley, S. F., and Pecccerillo, A., 1992, Potassic and ultrapotassic magmas and their origin: Lithos, v. 28, p. 181–185.

Frey, F. A., Dreen, D. H., and Roy, S. D., 1978, Integrated models for basalt petrogenesis: A study of quartz tholeiites to olivine melilitites from SE Australia utilizing geochemical and experimental petrological data: Journal of Petrology, v. 19, p. 463–513.

Gao, S., Lin, W. L., Qiu, Y. M., Zhou, L., Hartmann, G., and Simon, K., 1999, Contrasting geochemical and Sm-Nd isotopic compositions of Archean metasediments from the Kongling high-grade terrain of the Yangtze craton: Evidence for cratonic evolution and redistribution of REE during crustal anatexis: Geochimica et Cosmochimica Acta, v. 63, p. 2071–2078.

Gilder, S. A, Gill, J., Coe, R. S., Zhao, X., Liu, Z., Wang, G., Yuan, K., Liu, W., Kuang, G., and Wu, H., 1996, Isotopic and paleomagnetic constraints on the Mesozoic tectonic evolution of South China: Journal of Geophysical Research, v. 101, p. 16,137–16,154.

Guo, F., Fan, W. M., Lin, G., and Wu, Y. L., 1997a, Sm-Nd dating and petrogenesis of Mesozoic gabbro xenolith in Daoxian County, Hunan Province: Chinese Science Bulletin, v. 42, p. 1661–1663.

Guo, F., Fan, W. M., Lin, G., and Wu, Y. L., 1997b, Petrological characteristics and dating on gneiss xenoliths in Mesozoic basalts in Huziyan, Daoxian region, Hunan Province: Journal of Changchun College of Geology, v. 27, p. 41–46 (in Chinese with English summary).

HBGMR (Hunan Bureau of Geology and Mineral Resources), 1988, Regional geology of Hunan Province: Beijing, China, Geological Press, 534 p. (in Chinese with English summary).

Hegner, E., Kolbl-Ebert, M., and Loeschke, J., 1998, Post-collisional Variscan lamprophyres Black Forest, Germany: $^{40}Ar/^{39}Ar$ phlogopite dating, Nd, Pb, Sr isotope, and trace element characteristics: Lithos, v. 45, p. 395–411.

Holm, P. M., and Munksgard, N. C., 1982, Evidence for mantle metasomatism: An oxygen and strontium isotope study of the Vulsini district, central Italy: Earth and Planetary Science Letters, v. 60, p. 376–388.

Hsü, K. J., Li, J., Chen, H., Wang, Q. C., Sun, S., and Sengör, A., 1990, Tectonics of South China: Key to understanding West Pacific geology: Tectonophysics, v. 183, p. 9–39.

Hsü, K. J, Sun, S., Li, J., Chen, H. H., Pen, H. P., and Sengör, A., 1988, Mesozoic overthrust tectonics in South China: Geology, v. 16, p. 418–421.

Huang, C., 1977, Basic features of the tectonic structure of China: International Geology Review, v. 5, p. 289–320.

Jia, B. H., 1994, Tectonic deformation of the Xuefeng uplift area in Hunan: Regional Geology of China, p. 65–71 (in Chinese with English summary).

Joplin, G. A., 1968, The shoshonite association: A review: Journal of the Geological Society of Australia, v. 15, p. 275–294.

Leat, P. T., Thompson, R. N., and Morrison, M. A., 1988, Silicic magma derived by fractional-crystallization from Miocene minette, Elkhead Mountain, Colorado: Mineralogical Magazine, v. 52, p. 577.

Li, X. H., 1990, Preliminary discussion on the genesis of intermediate-basic veins from Zhuguangshan intrusion: Constraints from Sr, Nd and O isotopes: Chinese Science Bulletin, v. 35, p. 1247–1249.

Li, X. H., 2000, Cretaceous magmatism and lithospheric extension in southeast China: Journal of Asian Earth Sciences, v. 18, 293–305.

Li, X. H., Chen, Z. G., Liu, D. Y., and Li, W, X., 2003, Jurassic gabbro-granite-syenite suites from southern Jiangxi Province, SE China: Age, origin, and tectonic significance: International Geology Review, v. 45, p. 898–921.

Li, X. H., Chung, S. L., Zhou, H. W., Lo, C. H., Liu, Y., and Chen, C. H., 2004, Jurassic intraplate magmatism in southern Hunan-eastern Guangxi: $^{40}Ar/^{39}Ar$ dating, geochemistry, Sr-Nd isotopes, and implications for tectonic evolution of SE China, *in* Malpas, J., Fletcher, C. J., Aitchison, J. C., and Ali, J., eds., Aspects of the tectonic evolution of China: Geological Society of London Special Publication, v. 226, p. 3–216.

Li, X. H., Zhou, H. W., and Liu, Y., 1999, Shoshonitic intrusive suite in SE Guangxi: Petrology and geochronology: Chinese Science Bulletin, v. 44, p. 1992–1998.

Li, X. H., Zhou, H. W., Liu, Y., Lee, C. Y., Chen, Z. H., Yu, J. S., and Cui, X. L., 2000, Mesozoic shoshonitic intrusives in the Yangchun basin, western Guangdong, and their tectonic significance: Petrology and isotope geochronology: Geochimica, v. 29, p. 513–520 (in Chinese with English summary).

Li, Z. X., 1998, Tectonic evolution of the major East Asian lithospheric blocks since mid-Proterozoic—a synthesis, *in* Martin, F. J., Chung, S. L., Lo, C. H., and Lee, T. Y., eds., Mantle dynamics and plate interactions in East Asia: Washington, DC, American Geophysical Union, p. 221–243.

Liang, X. Q., Fan, W. M., Lin, G., and Wang, Y. J., 1999, On the Mesozoic continental activation and its multiple dynamics system: Geotectonica and Metallogenia, v. 23, p. 378–380 (in Chinese with English summary).

Lin, W., Faure, M., Monie, P., Scharer, U., Zhang, L., and Sun, Y., 2000, Tectonic of SE China: New insights from the Lushan massif (Jiangxi Province): Tectonics, v. 19, p. 852–871.

Lin, W., Faure, M., Sun, Y., Shu, L. S., and Wang, Q. C., 2001, Compression to extension switch during the Middle Triassic orogeny of Eastern China: The case study of the Jiulingshan massif in the southern foreland of the Dabieshan: Journal of Asian Earth Sciences, v. 20, p. 31–43.

Liu, Y., Liu, H. C., and Li, X. H., 1996, Simultaneous and precise determination of 40 trace elements using ICP-MS: Geochimica, v. 25, p. 552-558 (in Chinese with English).

McCulloch, M. T., Jaques, A. L., Nelson, D. R., and Lewis, J. D., 1983, Nd and Sr isotopes in kimberlites and lamproites from western Australia: An enriched mantle origin: Nature, v. 302, p. 400–403.

Mehdizadeh, H., Liotard, J. M., and Dautriac, J. M., 2002, Geochemical characteristics of an intracontinental shoshonitic association: The example of the Damavand volcano, Iran: Lithos, v. 334, p. 111–117.

Morrison, G. W., 1980, Characteristiccs and tectonic setting of the shoshonite rock association: Lithos, v. 13, p. 97–108.

Muller, D., and Groves, D. I., 1993, Direct and indirect associations between potassic igneous rocks, shoshonites, and gold-copper deposits: Ore Geology Reviews, v. 8, p. 383–406.

Muller, D., and Groves, D. I., 1995, Potassic igneous rocks and associated gold-copper mineralization: Berlin, Germany, Springer-Verlag, 210 p.

Muller, D., Rock, N. M. S., and Groves, D. I., 1992, Geochemical discrimination between shoshonitic and potassic volcanic rocks from different tectonic settings, a pilot study: Mineralogy and Petrology, v. 46, p. 259–289.

Nelson, D. R., McCulloch, M. T., and Sun, S. S., 1986, The origins of ultrapotassic rocks as inferred from Sr, Nd, and Pb isotopes: Geochimica et Cosmochimica Acta, v. 50, p. 231–245.

Pearce, J. A., 1982, Trace element characteristics of lavas from destructive plate boundaries, *in* Thorpe, R. S., ed., Andesites: New York, NY, Wiley, p. 525–548.

Peccerillo, A., 1985, Roman comagmatic province (central Italy): Evidence for subduction-related magma genesis: Geology, v. 3, p. 103–106.

Peccerillo, A., 1998, Relationships between ultrapotassic and carbonate-rich volcanic rocks in central Italy: Petrogenetic and geodynamic implications: Lithos, v. 43, p. 267–279.

Peccerillo, A., and Taylor, S. R., 1976, Geochemistry of Eocene calc-alkaline volcanic rocks from Kastamawarea, northern Turkey: Contributions to Mineralogy and Petrology, v. 58, p. 63–81.

Perfit, M. R., Gust, D. A., Bence, A. E., Arculus, R. J., and Taylor, S. R., 1980, Chemical characteristics of island-arc basalts: Implications for mantle sources: Chemical Geology, v. 30, p. 227–256.

Ren, J. S., Jiang, C. F., and Zhang, Z. K., 1980, Tectonics of China and its evolution: Beijing, China, Science Press, 160 p. (in Chinese with English summary).

Rogers, N. W., DeMulder, M., and Hawkesworth, C. J., 1992, An enriched mantle source for potassic basanites: Evidence from Karisimbi volcano, Virunga volcanic province, Rwanda: Contributions to Mineralogy and Petrology, v. 111, p. 543–556.

Rogers, N. W., Hawkesworth, C. J., and Mattey, D. P., 1987, Sediment subduction and the source of potassium in orogenic leucitites: Geology, v. 15, p. 451–453.

Rogers, N. W., Hawkesworth, C. J., Parker, R. J. and Marsh, J. S., 1985, The geochemistry of potassic lavas from Vulsini, Central Italy and implications for the evolution of mantle enrichment processes beneath the Roman region: Contributions to Mineralogy and Petrology, v. 90, p. 244–257.

Rogers, N. W., James, D., and Kelley, S. P., 1998, The generation of potassic lavas from the eastern Virunga Province, Rwanda: Journal of Petrology, v. 39, p. 1223–1247.

Rowley, D. B., Ziegler, A. M. and Gyou, N., 1989, Comment on Mesozoic overthrust tectonics in South China: Geology, v. 17, p. 384–386.

Rudnick, R. L., and Fountain, D. M., 1995, Nature and composition of the continental crust: A lower crustal perspective: Reviews of Geophysics, v. 33, p. 267–309.

Shen, W. Z., Ling, H. F., Li, W. X. and Wang, D. Z., 1998, Sr and Nd isotope of Mesozoic granitoids in Jiangxi Province: Chinese Science Bulletin, v. 43, p. 2653–2657.

Shu, L., Sun, Y., Wang, D., Faure, M., Charvet, J., Monie, P., 1998, Mesozoic extensional tectonics of the Wugongshan, in South China: Science in China (Series D), v. 28 (5), p. 431–438 (in Chinese).

Shui, T., 1987, Tectonic framework of Southeastern continental basement: Science in China (Series B), v. 4, p. 414–422 (in Chinese).

Sun, S. S, and McDonough, W. F., 1989, Chemical and isotopic systematics of oceanic basalts: Implications for mantle composition and processes, *in* Saunders, A. D., and Norry, M., eds., Magmatism in the ocean basins: Geological Society of London, Special Publication, v. 42, p. 528–548.

Taylor, S. R., and McLenann, S. M., 1985, The continental crust, its composition and evolution: Oxford, UK: Blackwell, 312 p.

Turner, S., Arnaud, N., Liu, J., Rogers, N., Hawkesworth, C., Harris, N., and Kelley, S., 1996, Post-collisional, shoshonitic volcanism on the Tibetan Plateau: Implications for convective thinning of the lithosphere and the source of ocean island basalts: Journal of Petrology, v. 37, p. 45–71.

Vollmer, R., 1977, Isotopic evidence for genetic relations between acid and alkaline rocks in Italy: Contributions to Mineralogy and Petrology, v. 60, p. 109–118.

Wang, H. Z., 1986, Geotectonic development of China, *in* Yang, Z. Y., Cheng, Y. Q., and Wang, H. Z., eds., The Geology of China: Oxford Monographs in Geology and Geophysics, v. 3, p. 235–275.

Wang, Q., Zhao, Z., Jian, P., Bao, Z., Xiong, X., and Ma, J., 2003, SHRIMP U-Pb zircon geochronology of Yangfang aegiriteaugite syenite in Wuyi Mountains of South China and its tectonic implications: Chinese Science Bulletin, v. 48, p. 2241–2247.

Wang, Y. J., Fan, W. M., and Guo, F., 2003a, Geochemistry of Early Mesozoic potassium-rich diorites-granodiorites in southeastern Hunan Province, South China: Petrogenesis and tectonic implications: Geochemical Journal, v. 37, p. 427–448.

Wang, Y. J., Fan, W. M., Guo, F., and Li, H. M., 2001, U-Pb dating of Mesozoic granodioritic intrusions in southeastern Hunan Province and its petrogenetic implication: Science in China (series D), v. 31, p. 745–751 (in Chinese).

Wang, Y. J., Fan, W. M., Guo, F., Peng, T. P., and Li, C. W., 2003b, Geochemistry of Mesozoic mafic rocks adjacent to the Chenzhou-Linwu Fault, South China: Implication for the lithospheric boundary between the Yangtze and Cathaysian Blocks: International Geology Review, v. 45, p. 263–286.

Weaver, B. L., 1991, The origin of ocean island basalt end-member composition: Trace element and isotopic constraints: Earth and Planetary Science Letters, v. 104, p. 381–397.

Wilkinson, J. F., and Le Maitre, R. W., 1987, Upper mantle amphiboles and micas and TiO_2, K_2O, P_2O_5 abundances and 100Mg/($Mg+Fe^{2+}$) ratios of common basalts and andesites: Implications for modal mantle metasomatism and undepleted mantle composition: Journal of Petrology, v. 28, p. 37–73.

Williams, H., Turner, S., Kelley, S., and Harris, N., 2001, Age and composition of dikes in southern Tibet: New constraints on the timing of east-west extension and its relationship to post-collisional magmatism: Geology, v. 29, p. 339–342.

Williams, H., Turner, S., Pearce, J., Kelley, S., and Harris, N., 2004, Nature of the source regions for post-collisional, potassic magmatism in southern and northern Tibet from geochemical variations and inverse trace element modelling: Journal of Petrology, v. 45, p. 555–607.

Winchester, J. A., and Floyd, P. A., 1976, Geochemical magma type discrimination: Application to altered and metamorphosed basic igneous rocks: Earth and Planetary Science Letters, v. 28, p. 459–469.

Wyborn, D., 1992, The tectonic significance of Ordovician magmatism in the eastern Lachlan Fold Belt: Tectonophysics, v. 214, p. 177–192.

Zhao, Z. H., Bao, Z. W., and Zhang, B. Y., 1998, The geochemistry of Mesozoic basalts in south Hunnan Province, South China: Science in China (Series D), v. 28, p. 7–14.

Zhi, X. C., 1990, Trace element geochemistry of tertiary continental alkalic basalt from Liuhe-Yizheng, Jiangsu Province: Acta Petrologica Sinica, v. 2, p. 30–42 (in Chinese with English summary).

Zhou, X. M. and Li, W. X., 2000, Origin of Late Mesozoic igneous rocks in southeastern China: Implications for lithosphere subduction and underplating of mafic magmas: Tectonophysics, v. 326, p. 269–287.

Zhou, X. M., Zhou, H. B., Yang, J. D., and Wang, Y. X., 1989, Sm-Nd ages of Fuchuan ophiolite in Anhui Province and its geological significance: Chinese Science Bulletin, v. 34, p. 1243–1245 (in Chinese).

Zhou, X. M., and Zhu, Y. E., 1993, Petrological characteristics of Neoproterozoic collisional orogenic belt and suture belt in southeastern, China, *in* Li, J. L., ed.-in-chief, Lithospheric structure of southeastern China: Continental and geological evolution: Beijing, China, Metallurgy Industry Press, p. 60–68 (in Chinese).